PE/OMMT Nanocomposites Catalyzed by the OMMT-Intercalated Et[Ind]$_2$ZrCl$_2$ in Slurry Polymerization: Effects of Organic Solvent on Ethylene Polymerization Behaviors and the Nanocomposite Structures

Ying-Juan Huang,[1,2] Ya-Wei Qin,[1,2] Jin-Yong Dong[1]

[1]*CAS Key Laboratory of Engineering Plastics, Joint Laboratory of Polymer Science and Materials, Institute of Chemistry, The Chinese Academy of Sciences, Beijing 100190, China*
[2]*Graduate School of the Chinese Academy of Sciences, Beijing 100049, China*

Received 23 December 2009; accepted 10 March 2010
DOI 10.1002/app.32429
Published online 21 July 2010 in Wiley Online Library (wileyonlinelibrary.com).

ABSTRACT: *In situ* intercalative polymerization for ethylene monomers was carried out to produce PE-based hybrids through a slurry polymerization method. In this approach, organic solvent for olefin polymerization was found to be one of the most significant factors for the dispersion of the OMMT-intercalated Et[Ind]$_2$ZrCl$_2$ catalysts, which determines that whether olefin monomers polymerize is in a well-defined confinement environment or not. Understanding the olefin polymerization occurring in between the nanoscale silicate layers of OMMT as well as the corresponding structure of OMMT in an organic polymerization solvent is a critical step toward tailoring and characterizing nanocomposites formed by OMMT in a polyolefin matrix. As we know, the Et[Ind]$_2$ZrCl$_2$ catalyst and MAO are both better dissolved in toluene than that in hexane because of the larger polarity of toluene. Thus, in hexane the active sites of the OMMT/Et[Ind]$_2$ZrCl$_2$ catalyst exist in the silicate layers of OMMT and the PE chains grow in the middle of them, while in toluene the active specimens are exposed in the gel formed by the OMMT-intercalated catalyst with MAO, which cause that the PE chains propagated in the mixture liquids. Consequently, when hexane is selected as the polymerization solvent, the formed PE-based nanocomposites have a good dispersion of OMMT and the nanofiller content (TGA measurement residue at 600°C) is thus higher (>7.0 wt %). However, in toluene, most of the silicate layers of OMMT are agglomerated in the PE matrix. © 2010 Wiley Periodicals, Inc. J Appl Polym Sci 119: 190–200, 2011

Key words: *in situ* intercalative polymerization; slurry polymerization; polyethylene (PE); OMMT/Et[Ind]$_2$ZrCl$_2$; nanocomposites

INTRODUCTION

Intensive research on polymer-clay nanocomposites in organic–inorganic hybrids has been receiving considerable attention because clay nanocomposites have a high modulus, dimensional stability, low gas permeability, and antiflammability,[1,2] which are usually too difficult to access by traditional micrometer-scale inorganic fillers.[3,4] These enhanced properties result from nanoscale dispersions of the silicate layers in polymer matrixes and the subsequent interactions between the clays and polymers.[5,6]

In the case of polyolefin/clay nanocomposites, it is very tough to adopt the direct polymer intercalation (including melt and solution intercalations) to disperse MMT into nanoscale silicate layers in polyolefin matrix due to the wide discrepancy between the polar clay filler and nonpolar polyolefin.[7] However, *in situ* intercalative polymerization has been as an effective approach to prepare this type of nanocomposites catalyzed by the OMMT-intercalated transition metal olefin polymerization catalysts, such as Ziegler-Natta, metallocene, and postmetallocene.[8] Because monomers of *in situ* polymerization can penetrate the interlayer spaces of clays more easily than polymers or macromolecules, this approach has the advantage of bypassing the thermodynamic obstacles associated with direct polymer intercalation.[9,10] In fact, the *in situ* polymerization technique has been widely applied to prepare polyolefin/clay nanocomposites.[11,12] There is abundant evidence available to show it is more desirable in terms of effectiveness to form nanocomposite structures than a melt or solution polymer intercalation assisted by a functional polyolefin compatibilizer.[13,14] Sivaram and coworkers reported *in situ* polymerization of ethylene with the 2,6-bis[1-(2,6-diisopropylphenylimino)ethyl] pyridineiron(II) dichloride catalyst supported on clay and obtained a series of PE/OMMT nanocomposites with different degree of exfoliation of MMT.[15] Tang and coworkers also used

Correspondence to: J.-Y. Dong (jydong@iccas.ac.cn).
Contract grant sponsor: National Science Foundation of China; contract grant number: 20734002.

zirconocene catalysts entrapped inside the modified montmorillonite to prepare polyethylene/OMMT nanocomposites.[16,17]

The *in situ* intercalative polymerization of olefin monomers is generally carried out through a slurry polymerization method as follows: (1) olefin monomers dissolve in an organic polymerization solvent such as toluene, hexane, heptane, etc.; (2) OMMT-intercalated olefin polymerization catalysts are dispersed in the above solvents; (3) olefin monomers get inside the interlayer spaces of OMMT to approach to the active sites and start to polymerize and propagate into polyolefin chains. In other words, during the slurry polymerization process, organic solvents act as a medium between olefin monomers and OMMT-intercalated catalysts. Consequently, the dispersion degree of OMMT-intercalated catalysts in organic polymerization solvents affects the final state of OMMT with exfoliation or agglomeration in polyolefin matrixes. Some researchers have ever used Hansen solubility parameters, $\delta_t^2 = \delta_d^2 + \delta_p^2 + \delta_h^2$, to explain the dispersion of organically modified clays (organoclay) in organic solvents.[18,19] The dispersive components of the solvents (δ_d) greatly affect the degree of dispersion because of the hydrophobic modifier molecules that covered the organoclays. The polar components (δ_p) and the hydrogen components (δ_h) are important for the dispersion or exfoliation of natural clay. Smectite clays have the properties of cation exchange, intercalation of molecules and swelling in solvents.[20] For example, sodium montmorillonite (MMT), which is a type of smectite clay, expands the interlayer spaces when immersed in a hydrophilic solvent such as water. Thus, the exfoliation degree of organoclays depends on the physico–chemical properties of solvents. Ho et al. used Hansen's solubility parameters to successfully analyze the correlation between the degree of exfoliation of organoclay (C15A) and the solvent in which clay platelets were dispersed/mixed.[21] They concluded that δ_d of the solvent is the primary factor determining whether C15A clay platelets remain suspended, whereas δ_p and δ_h affect the tactoid formation/structure of the platelets in the dispersion. Chung and coworkers analyzed the dispersion states and the basal spacing expansion of natural MMT in organic liquids utilizing Hansen's solubility parameters.[22] And they successfully synthesized polymer/MMT nanocomposites with a good dispersion of MMT by the *in situ* polymerization method.

Despite the claimed successes of the *in situ* polymerization method, according to the literatures,[12,15,23,24] it is found that when the weight content of clay is high (usually above 7 wt %), the silicate layers of clay generally agglomerate in the polyolefin matrix. Of course, this final structure of OMMT in PE-based hybrids has a relationship with the nature of inorganic supports and olefin polymerization catalytic systems, and experimental polymerization conditions (including the polymerization solvent, temperature, pressure, time, and the concentration of the catalyst so on). In our previous study, we used a functional surfactant to modify the Na-montmorillonite and promote efficiency of preparing iPP/MMT nanocomposites by the *in situ* polymerization technique. A series of iPP/MMT nanocomposites containing completely disordered MMT at a loading range of 1.0–6.7 wt % (TGA measurement residue at 600°C) were obtained in high yields.[25] Recently, Tritto and coworkers prepared highly filled (>9 wt %) PE-based hybrids with a homogeneous distribution of clay, and they further produced low-filled and well-dispersed PE/clay nanocomposites by *in situ* intercalative polymerization.[23,24] They concluded that it was possible to tune the final properties of PE as well as the morphology of nanocomposites by varying the nature of inorganic supports and 2,6-bis(imnio)pyridyl iron(II) catalytic systems, the clay pretreatment, and experimental polymerization conditions.

To produce exfoliated polyolefin/OMMT nanocomposites by *in situ* polymerization successfully, we should therefore understand the olefin polymerization in between the nanoscale silicate layers of OMMT as well as the corresponding structure of OMMT in an organic polymerization solvent, which is a critical step toward tailoring and characterizing nanocomposites formed by OMMT in polyolefin matrixes. Consequently, organic solvent used for the slurry polymerization of olefin monomers was one of the most significant factors for the dispersion of OMMT-intercalated catalysts.

The motivation of our study is to explore the correlation between the dispersion state of OMMT and the properties of organic solvents for ethylene polymerization, and its role on *in situ* polymerization technique adopted. In this article, hexane and toluene were selected as polymerization solvents in slurry polymerization using OMMT-intercalated $Et[Ind]_2ZrCl_2$ catalyst. We paid particular attention on the following: (i) dispersion and swelling of OMMT, MAO, OMMT/$Et[Ind]_2ZrCl_2$, and OMMT/$Et[Ind]_2ZrCl_2$ with MAO in hexane and toluene; (ii) kinetic profiles of ethylene polymerization catalyzed by $Et[Ind]_2ZrCl_2$/OMMT in both solvents with different polarity; (iii) influence of parameters, such as the polymerization solvent, time and temperature on preparing nanocomposites with improved filler dispersion within continuous PE matrix.

Thermal behaviors of PE/OMMT nanocomposites were investigated by thermogravimetric analysis (TGA) and differential scanning calorimetry (DSC). Their structure and morphology were thoroughly analyzed by wide angle X-ray diffraction (WAXD) and transmission electron microscopy (TEM).

EXPERIMENTAL

Materials

All O_2-and moisture-sensitive manipulations were carried out inside an argon-filled vacuum atmosphere dry-box equipped with a dry train. Chemically pure-grade toluene and hexane were deoxygenated by argon purge before being refluxed for 48 h and distilled over sodium. The surfactant, dimethyloctadecyl hydroxylethyl ammonium, was purchased from Beijng Jingxi Chemical Factory. Methylaluminoxane (MAO) (1.4 *M* in toluene) was purchased from Albermarle and used as received. Et[Ind]$_2$ZrCl$_2$ was purchased from Aldrich.

Polymerization-grade ethylene was supplied by Yanshan Petrochemical of China. The original Na-MMT was produced by Qinghe Chemical Plant (China) with a cation exchange capacity (CEC) of 100 mequiv. (100 g)$^{-1}$. Na-MMT was modified by a surfactant of dimethyloctadecylhydroxylethyl ammonium ($C_{22}H_{48}N_2O_4$). The organic content of OMMT was 20.8 wt %.

Preparation of the OMMT-intercalated catalyst

One-hundred milliliter of toluene was added to 5.0 g of OMMT at 60°C in a 500 mL three-necked flask. Then the mixture was stirred for 2 h, followed by the addition of 16.0 mL of MAO. The reaction was stirred for 8 h, and 0.502 mmol of *rac*-Et[Ind]$_2$ZrCl$_2$ in MAO solution ([Al]/[Zr] = 100) was added by syringe into the flask. The reaction was allowed to proceed for 16 h, then the reactants were subjected to filtration, washing with toluene (5 × 50 mL), and drying under vacuum at 60°C to give the OMMT-intercalated Et[Ind]$_2$ZrCl$_2$ catalyst (OMMT/Et[Ind]$_2$ZrCl$_2$) as a gray powder.

Dispersion and swelling of OMMT, MAO, OMMT/Et[Ind]$_2$ZrCl$_2$ and OMMT/Et[Ind]$_2$ZrCl$_2$+MAO in hexane and toluene

The required amount of four samples: OMMT, MAO, OMMT/ Et[Ind]$_2$ZrCl$_2$ (Cat.), and OMMT/ Et[Ind]$_2$ZrCl$_2$ (Cat.) + MAO, was separately added into test tubes containing 10 mL hexane or toluene at room temperature, as shown in Table I. Then the liquid mixtures were dispersed by ultrasonic dispersion for 4 h. Finally, the states of dispersion of all samples were investigated after they were placed still for 48 h.

Preparation of PE/OMMT nanocomposites

The polymerization reactions were carried out with a Parr stainless steel autoclave reactor equipped with a mechanical stirrer. In a typical reaction (entry TE6 in Table IV), 100 mL of toluene was introduced into the reactor. The reactor was then filled with ethylene under a constant pressure of 0.5 MPa. After the reactor had been heated to 50°C, the powdery Et[Ind]$_2$ZrCl$_2$/OMMT catalyst (0.302 g,) was added into the vigorously stirred liquid mixture saturated with ethylene. The polymerization reaction was initiated by charging MAO (2.3 mL, 3.3 mmol) into the reactor using a syringe. After 30 min, the polymerization was quenched by 20 mL of acidified ethanol (containing 10% HCl). The polymer product was collected by filtration and repeatedly washed with ethanol and distilled water. After drying under vacuum at 60°C for 24 h, 4.03 g of polymer product was obtained as white powder (PE/OMMT).

TABLE I
The Amounts of Four Samples: OMMT, MAO, Cat., Cat.+MAO

Solvent	OMMT (g)	MAO (mL)	Cat. (g)	Cat. (g) +MAO (mL)
Hexane	0.100	0.5	0.100	0.101 + 0.5
Toluene	0.100	0.5	0.100	0.102 + 0.5

Characterization

The melting temperatures of the polymers were measured by DSC using a Perkin–Elmer Pyris 1 instrument. All specimens were heated from 50 to 180°C at heating rate of 10°C /min and kept for 5 min to eliminate the thermal history. The melt and crystallization behavior was then recorded at heating or cooling rate of 10°C/min. And the melt temperature (T_m) was determined at the second heating scan.

TGA was performed on a Perkin–Elmer TGA instrument in nitrogen atmosphere under a flow rate of 50 mL/min with a heating range of 50–700°C and a heating rate of 20°C/min. The inorganic content in the hybrid composites was determined by the residue observed at 600°C.

Wide-angle X-ray diffraction (WAXD) was performed on a D8 advance X-ray powder diffractometer (Bruker) with Cu Ka radiation (λ = 0.15406 nm) at a generator voltage of 40 kV and generator current of 40 mA. The scanned 2Θ range was from 1.5 to 40° with a scanning rate of 4°/min. The interlayer spacing (d001) of MMT was calculated in accordance with the Bragg equation: $2d\sin\Theta = \lambda$. The powder-polymerized samples were compressed at room temperature before being evaluated by WAXD.

Transmission electron microscopy (TEM) was carried out on a Jeol JEM2200FS transmission electron microscope using an acceleration voltage of 200 kV. Samples for TEM were prepared by embedding in

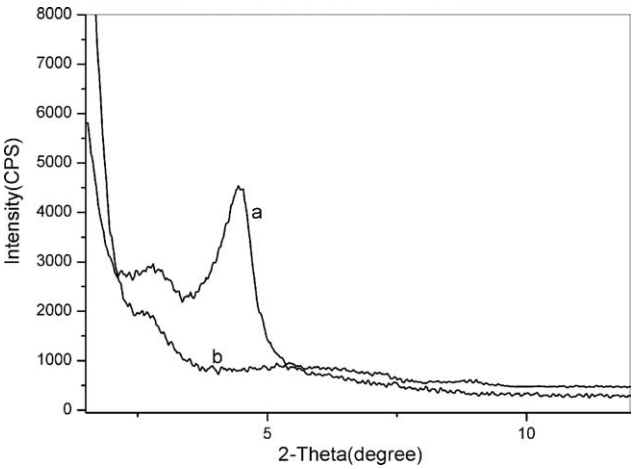

Figure 1 A comparison of WAXD patterns of (a) OMMT and (b) the OMMT-intercalated metallocene catalyst (Cat.).

epoxy resin at room temperature and microtomed into ultra-thin sections.

The molecular weight and molecular weight distribution of the polymers were determined by gel permeation chromatography (GPC) using a Waters Alliance GPC 2000 instrument equipped with a refractive index (RI) detector and a set of m-Styragel HT columns of 106, 105, 104, and 103 pore sizes in series. The measurement was performed at 150°C with 1,2,4-trichlorobenzene as the eluent with a flow rate of 0.7 mL/min. Narrow molecular weight polystyrene (PS) samples were used as standards for calibration. Before GPC of the polymers was conducted, the samples were extracted in xylene at 140°C. Approximately 300 mg of the PE-clay composites was placed in a packet made of two filter papers and submerged in xylene at 140°C. The clay inside the packet agglomerated. After 30 min, the packet was removed and hot xylene was poured into ethanol. Then, the precipitates were filtered and dried. This entire process was repeated again to ensure complete separation of PE from clay. Typically, the final weight of the polymer was approximately 100–150 mg.

RESULTS AND DISCUSSION

The OMMT-intercalated Et[Ind]$_2$ZrCl$_2$ catalyst

The OMMT-intercalated metallocene catalyst was prepared by treating OMMT successively with MAO and Et[Ind]$_2$ZrCl$_2$ in toluene. The obtained supported catalyst OMMT/Et[Ind]$_2$ZrCl$_2$ (Cat.) has been subjected to Zr and Al content measurement, to obtain values of 0.10 and 13.20 wt % (OMMT contains 9.08 wt % of measurable Al), respectively. Figure 1 shows the comparison of WAXD patterns of OMMT and OMMT/Et[Ind]$_2$ZrCl$_2$. In contrast to OMMT, there is a distinct shift of the (001) diffraction peak for the supported catalyst ($2\Theta = 2.68°$, with a secondary peak at 5.53°). And the peaks are obviously broad, indicating an effective intercalation of MAO and metallocene catalyst.[12]

Dispersion and swelling of OMMT, MAO, Cat., and Cat.+MAO in hexane or toluene

Dispersion and swelling are two important characters of clays in organic solvents. Hauser seems to first note that organic complexes of montmorillonite can swell extensively in organic solvents.[26] To elucidate the mechanism of swelling and gel formation of the organoclay complexes in binary organic liquid mixtures, Slabaugh studied the selective adsorption of the polar components and measured the heat of immersion.[27–29] These properties are correlated with the solvent polarity and organoclay gel strength only with the homologous series of alcohols. Moraru reported that the condition for the gel formation of alkylammonium montmorillonites in organic liquids is intracrystalline swelling and dispersion.[30] And gel formation also depends on the physico–chemical properties of the solvents.

To illustrate dispersions of organoclay complexes (OMMT, MAO, Cat., and Cat.+MAO) were separately dispersed in hexane and toluene with the aid of the ultrasonication and the dispersions were all allowed to settle for 48 h as mentioned in the experimental part. Figure 2 shows digital pictures of different dispersion results of all samples above in hexane or toluene. It's well known that MAO is poorly dispersed in hexane, while it can be well dissolved in toluene, seen in Figure 2.

From Figure 2, we can also observe that OMMT swells to 20–30 times of its original volume in toluene, which is larger than that in hexane. It can be interpreted by dispersion states of MMT in hexane and toluene according to the Hansen solubility

Figure 2 Dispersion and swelling profiles of OMMT, MAO, Cat. (Et[Ind]$_2$ZrCl$_2$/OMMT), Cat. + MAO in hexane and toluene, respectively.

TABLE II
Dispersion States of MMT in Organic Liquids and the Hansen Solubility Parameters[a]

Organic liquids	δ_d MPa$^{1/2}$	δ_p MPa$^{1/2}$	δ_h MPa$^{1/2}$	δ_t[b] MPa$^{1/2}$	H-bonding group	Dispersion state
Toluene	18.0	1.4	2.0	18.2	Poor	Precipitated
n-hexane	14.9	0	0	14.9	Poor	Precipitated

[a] All solubility parameter values are from Ref. [31] and the unit is MPa$^{1/2}$.
[b] $\delta_t^2 = \delta_d^2 + \delta_p^2 + \delta_h^2$ where δt is the total solubility parameter, δ_d is the dispersive component, δ_p is the polar component, and δ_h is the hydrogen-bonding component of the Hansen solubility parameters.

parameters, as shown in Table II.[31] The hydrogen component (δ_h) and the polar component (δ_p) are the primary parameters for the dispersion states and for the basal spacing expansion,[22] moreover, both δ_h value and δ_p value of toluene are higher than those of hexane. Thus, OMMT in toluene has a better swelling than that in hexane.

For OMMT/Et[Ind]$_2$ZrCl$_2$ (Cat.), it was found that Cat. dispersed in toluene was yellow due to the fact that Et[Ind]$_2$ZrCl$_2$ could sufficiently dissolve in toluene, while in hexane it was white. Because the organocomplexes and MAO in the silicate layers of the OMMT-intercalated catalyst are relatively easier to disperse in toluene than in hexane, sample Cat.+MAO in toluene displays a comparatively good swelling. Sample Cat.+MAO with inner and added MAO in toluene has the ability to swell and form a gel. However, it only swells in hexane.

WAXD analysis was employed to gain further insight into the capability of solvents to disperse OMMT complexes. WAXD patterns in both solvents were obtained under identical conditions (i.e., they were all recorded 48 h after the dispersions were prepared). Figure 3 shows WAXD patterns for all dispersion samples.

First, as a comparison and reference, WAXD patterns of OMMT and Cat. at their dry state also were measured and shown in Figure 3. From Figure 3(Aa), there is a distinct shift of the d_{001} peak for OMMT in hexane toward higher angle ($2\Theta = 4.56^\circ$) than that of dry OMMT ($2\Theta = 4.46^\circ$), and 020 and 060 diffraction peaks of OMMT in hexane are hardly any change at all. In other words, the d_{001} layer spacing of OMMT in hexane (1.93 nm) hardly changed compared with that for the corresponding OMMT at its dry state (1.98 nm). These were resulted from the fact that the hexane could be capable of solvating the hydrocarbon chain in the interlayer space of OMMT but could not interact with the polar surface of the platelet.[27] However, in toluene the corresponding d_{001} diffraction peak shifts to a lower angle ($2\Theta = 2.36^\circ$, a secondary peak at $2\Theta = 4.48^\circ$), seen in Figure 3(Ba), implying that the toluene molecules immersed into the interlayers of OMMT and induced to enlarge the d_{001} layer spacing (3.74 nm). Combined with Figure 2, this is in accordance with Muzny's reports[32] that the organoclay (C15A) could disperse well, but did not fully exfoliate in toluene. What's more, compared to WAXD patterns of dry OMMT and OMMT in hexane [Fig. 3(Aa)], there is a broader peak at the angle of 15–19° in the curve of OMMT in toluene, and the 020 peak presents reduced diffraction intensity, seen in Figure 3(Ba). The reason for this may be that the toluene molecules may be trapped by their interaction with the polar adsorbate and the ammonium ion to penetrate the crystalline lattice of OMMT and destroy the crystal.[28]

As expected, MAO in hexane sample [Fig. 3(Ab)] showed no peak at the angle from 1.5 to 40°, while sample MAO in toluene [Fig. 3(Bb)] appears the broad peak at $2\Theta = 15$–20°, suggesting that MAO can well dissolve in toluene comparable to hexane.

The 001 diffraction peak in the WAXD pattern of sample Cat. in hexane [Fig. 3(Ac)] was distinct at the angle of 4.46°, and the corresponding d_{001} distance is 1.98 nm. However, the catalyst in toluene sample [Fig. 3(Bc)] shows no 001 diffraction peaks, indicating that the average interlayer spacing of OMMT was larger than 5.8 nm according to the Bragg equation. And it appears a broad peak at the angle from 15 to 20° and both 020 and 060 peaks show reduced diffraction intensities if compared with Cat. at its dry state, which is caused by the two reasons: (1) the toluene molecules penetrated into the crystalline lattice of OMMT and destroyed the crystal; (2) MAO existing in the interlayer of OMMT is well solvated by the toluene.

For sample Cat. with addition of MAO in hexane, its WAXD pattern [Fig. 3(Ad)] displays a broader (001) diffraction peak at $2\Theta = 3$–6° in contrast to that of Cat. without addition of MAO in hexane [Fig. 3(Ac)]. The reason for this may be that the interaction between the MAO added and the active species of Et[Ind]$_2$ZrCl$_2$ existing in the silicate layers of OMMT destroyed the layer order. But for sample Cat. with addition of MAO in toluene, the corresponding peak [Fig. 3(Bd)] disappears, which is in concord with the Cat. without additional MAO sample [Fig. 3(Bc)]. So we can conclude that the silicate layers of the OMMT-intercalated catalysts are relatively well disordered in toluene.

To illustrate the effect of solvents on the dispersion state of OMMT in the OMMT-intercalated

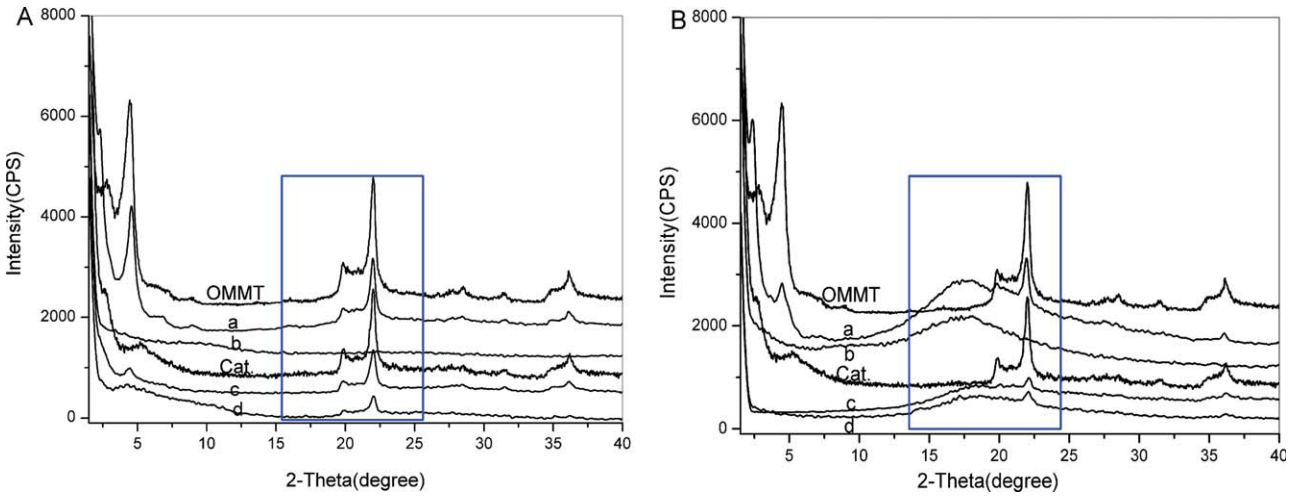

Figure 3 WAXD patterns of (a) OMMT, (b) MAO, (c) Cat., and (d) Cat.+MAO with dispersion in (A) hexane and (B) toluene, respectively. The patterns of samples were measured at their wet state. WAXD patterns of OMMT and Cat. were measured at their dry state.

catalyst in detail, we simulated the polymerization process in the absence of ethylene inside an argon-filled with vacuum atmosphere dry-box equipped with a dry train and analyzed Zr contents as following steps. MAO (2.3 mL) and OMMT/Et[Ind]$_2$ZrCl$_2$ (0.3000 g) were in turn added into a 250 mL three-necked flask containing 100 mL hexane or 100 mL toluene at 50°C. (i) The mixtures were stirred for 30 min and then the stirring was stopped. In the mean time, 30 mL of the liquid mixtures were taken out to measure the Zr content in the fluids by titration. The measured results were presented in Table III. As we predicted, Zr concentrations in hexane liquids (2.96×10^{-5} mol/L) and in toluene liquids (3.04×10^{-5} mol/L) are the same as the added Zr content in the feed (3.12×10^{-5} mol/L). (ii) 50 mL of upper liquids were taken out to be centrifuged at 200 rpm for 5 min after the mixtures were placed still for 1 h, and then 40 mL of upper liquids were used to measure the Zr content again, as seen in Table III. The Zr concentration in hexane liquids (0.88×10^{-5} mol/L) was much lower than that in toluene liquids (3.02×10^{-5} mol/L) and the calculating concentration of Zr added into the feed (3.12×10^{-5} mol/L). By contrast, the active sites in toluene were seen to exhibit relatively long-term stability comparable to that in hexane. Et[Ind]$_2$ZrCl$_2$ and MAO are both well dissolved in toluene compared to hexane. Thus, we consider that Et[Ind]$_2$ZrCl$_2$ active sites embedded in large MAO were easier to expose in toluene than in hexane facilitating the ethylene molecules approaching. That is to say, in toluene most of active sites were exposed in the toluene gel departing from the confinement of the silicate layers of OMMT, and in hexane most of them were in between the silicate layers of OMMT. Consequently, we deduced that the polymer chains grow within the clay galleries and separate them in hexane as polymerization solvent. (iii) Finally the residue mixtures were dried under vacuum at 50°C to remove the organic solvent and the dried powder was subjected to Zr content measurement. The Zr content from hexane (0.104 wt %) is almost no change in that from toluene (0.099 wt %), which is in accord with the value of the Zr content in the original OMMT-intercalated catalyst (0.10 wt% seen in Table III).

Kinetic profiles of ethylene polymerization with OMMT/Et[Ind]$_2$ZrCl$_2$ in hexane and toluene

Ethylene polymerization in hexane and toluene catalyzed by OMMT/Et[Ind]$_2$ZrCl$_2$ was investigated in detail to study the effect of organic solvent on the polymerization process in the well-defined confinement environment. Figure 4 presents the kinetic curves of ethylene polymerization in hexane [Fig. 4(A)] and in toluene [Fig. 4(B)] at different reaction conditions. Under reaction temperature at 70°C and pressure at 0.5 MPa in hexane [Fig. 4(A)], at the beginning of polymerization, absorbed C_2H_4 amount accelerated rapidly and reached

TABLE III
Results of Zr Content Measurement With Different Treatment

Methods	Solvent	Zr
After stirring for 30 mins	Hexane	2.96×10^{-5} mol/L
	Toluene	3.04×10^{-5} mol/L
After placing still for 1 hour	Hexane	0.88×10^{-5} mol/L
	Toluene	3.02×10^{-5} mol/L
After drying under vacuum	Hexane	0.104 wt %
	Toluene	0.099 wt %
Theoretical calculating values in the feed	Hexane	3.12×10^{-5} mol/L
	Toluene	3.12×10^{-5} mol/L
Practical measurement values in dry catalyst	–	0.10 wt %

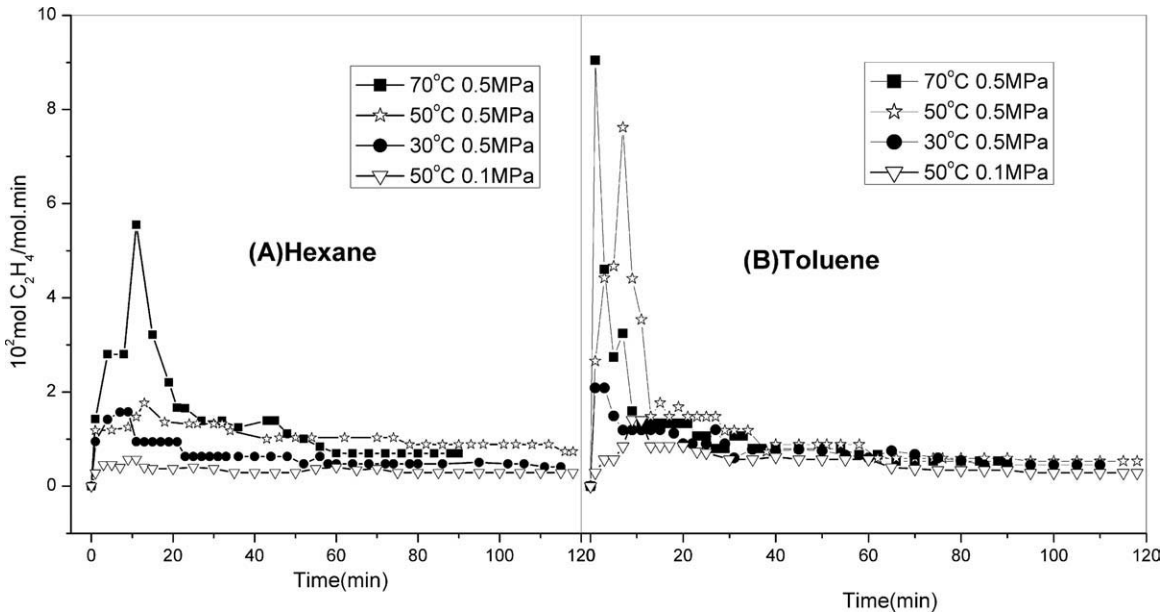

Figure 4 Kinetic profiles of ethylene polymerization with OMMT/Et[Ind]$_2$ZrCl$_2$ under different reaction conditions in hexane and toluene, respectively.

its maximum (5.8×10^2 mol C_2H_4/mol Zr min) at about 13 min. Then C_2H_4 amount started to decay and remained so slow after more than 40 min that it hardly changed until the polymerization was completed. However, at the similar reaction conditions in toluene, the absorbed C_2H_4 amount fleetly reached its maximum (9.1×10^2 mol C_2H_4/mol Zr min) with the reaction time of 5 min, which was earlier than that in hexane (13 min). This may be due to the fact that the polyethylene chains grow in the gel formed by the dispersion of OMMT/Et[Ind]$_2$ZrCl$_2$ and MAO in toluene, while in hexane they grow in between the silicate layers of OMMT , supported by the above analysis. The maximum value of the absorbed C_2H_4 amount in toluene is larger than that in hexane, which may be that the Cat. with MAO added in toluene is better dispersive than that in hexane and this gives more opportunity for ethylene molecules approaching to the active sites of the catalyst. Likewise, at the same reaction conditions other than organic solvents, the absorbed C_2H_4 maximum value in toluene is higher than the corresponding value in hexane. But whether in toluene or in hexane, the absorbed C_2H_4 value remains unchanged when the polymerization time is over 45 min. In the case of toluene, it is found that the absorbed C_2H_4 maximum amount augments with the rise in the polymerization temperature from 30 to 70°C and the polymerization pressure from 0.1 to 0.5 MPa.

Ethylene polymerization with OMMT/ Et[Ind]$_2$ZrCl$_2$ catalyst

Ethylene polymerization was performed with OMMT/Et[Ind]$_2$ZrCl$_2$ catalyst under different reaction conditions, and the results were summarized in Table IV and Figure 5. It displays the correlation between polymerization activity and reaction time. The catalytic activity of OMMT/Et[Ind]$_2$ZrCl$_2$ decreased rapidly within 45 min and remained almost no change after 45 min at 50°C whether in hexane or in toluene. But at 30°C in hexane, the catalytic activity for ethylene polymerization dropped off very slowly with increasing reaction time and exhibited a significant inferiority to that at 50°C. The reason may be that the low polymerization temperature is not conducive to the dispersion of OMMT/ Et[Ind]$_2$ZrCl$_2$ in hexane, which reduces the opportunities for ethylene molecules approaching into the active sites in between the OMMT lamellae interlayers. Under similar reaction conditions (same polymerization temperature and ethylene pressure, similar catalyst and cocatalyst amounts), the polymerization activity in toluene is obviously higher than that in hexane when the polymerization time is less than 15 min. But with the gradual increase of polymerization time over 15 min, the activity in toluene is slightly lower than that in hexane. In the early stage of polymerization, due to a good dispersion of OMMT-intercalated catalyst with MAO added in toluene, ethylene molecules gain more opportunities to approaching the active sites and so the polymerization activity are higher in toluene than that in hexane. With the polymerization proceeding, more and more polyethylenes are produced among the gallery of OMMT and the gallery distance increased.[12] The larger gallery distance of clay in turn favors diffusion of the monomer into the active sites and the propagation of the polyethylene

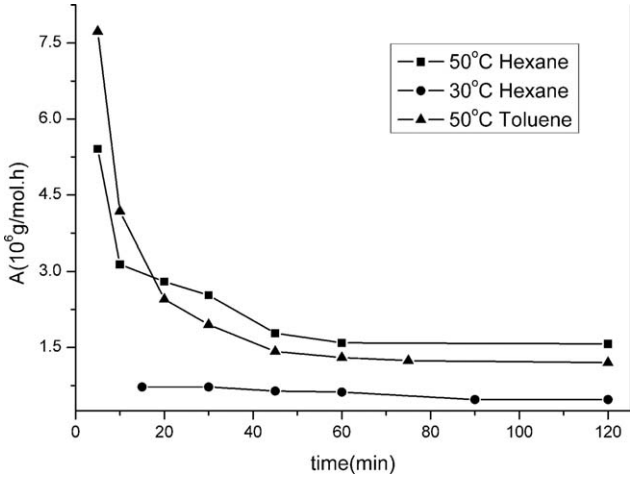

Figure 5 Activity of ethylene polymerization with OMMT/Et[Ind]$_2$ZrCl$_2$ versus the reaction time.

chain generated amid the gallery eventually destroys the laminated structure. When the exfoliation of the OMMT sheet occurs, the monomers can approach all active sites, and the polymerization activity remains unchanged when the reaction time is over 45 min. However, in toluene, most of the active specimens are in the gel formed by the OMMT/Et[Ind]$_2$ZrCl$_2$ catalyst dispersion in solvent and the polymer chains grow in the mixture liquids from the beginning to the end of polymerization. However, as the polyethylene chains propagate, the OMMT would result in a steric hindrance toward further growth of the polymer chains. So the ethylene polymerization activity in toluene is basically the same as that in hexane when the reaction time is over 45 min.

As expected, the yield of PE is improved upon the increase of polymerization time. Consequently, at higher polymerization time the OMMT content in PE nanocomposites significantly decreased both in toluene and in hexane.[12,25] Such an increase of reaction time lowers the OMMT content in PE/OMMT final products: sample HE1 (t = 5 min) has a clay content of 14.5 wt %, while sample HE7 (t = 120 min) has a content of 2.7 wt %. Because the polymerization temperature has a significant impact on the catalytic activity, highly filled (>7 wt % of OMMT content) PE/OMMT nanocomposites prepared from hexane are obtained at 30°C, higher than that at 50°C. As a result, by controlling the polymerization time and temperature, we have prepared a series of PE-based nanocomposites with OMMT at a loading range of 1.1–22.1 wt %.

Characterization of PE/OMMT nanocomposites

TGA and DSC analysis

The thermal properties of PE/OMMT nanocomposites were investigated by TGA and DSC, and the results were summarized in Table IV. For all PE/OMMT nanocomposites, the melting temperatures are equal or slightly differential. The trends were slightly different with the other reports in the literatures,[12,23,24] which could be caused by the different nature of the OMMT-intercalated catalysts (including the surface modifiers and the catalysts).

Figure 6 presents the DTG curves of PE/OMMT with different OMMT contents (sample HE8-HE13, seen in Table IV) and neat PE catalyzed by Et[Ind]$_2$ZrCl$_2$/MAO as a reference. DTG trace of sample HE8 with 22.1 wt % OMMT is characterized by a two-stage decomposition, which is obviously different from neat PE (only exhibiting a single narrow peak of degradation centered at 493°C). It displays two main decomposition peaks: one occurs at the range of 220–342°C and the other is at around 455°C. Low temperature weight loss is partially ascribed to the degradation of the organic modifier due to highly filled amount of OMMT in PE-based hybrid without exfoliation/disorder (seen in WAXD analysis section). The major peak at about 455°C is due to the degradation of polyethylene chains. However, compared to sample HE8, other nanocomposites show only one decomposition peak at higher temperature (> 455°C).

The degradation behavior of composites is obviously sensitive to the synthesis parameters. The nanocomposites produced from hexane as polymerization solvent at 30°C show a higher thermal stability because the amount of inorganic residue was lower in PE matrix. Such high temperature weight loss of sample HE10 with 14.2 wt % MMT and HE9 with 17.9 wt % MMT is at 485°C and around 472°C, respectively, which is lower than that of neat PE

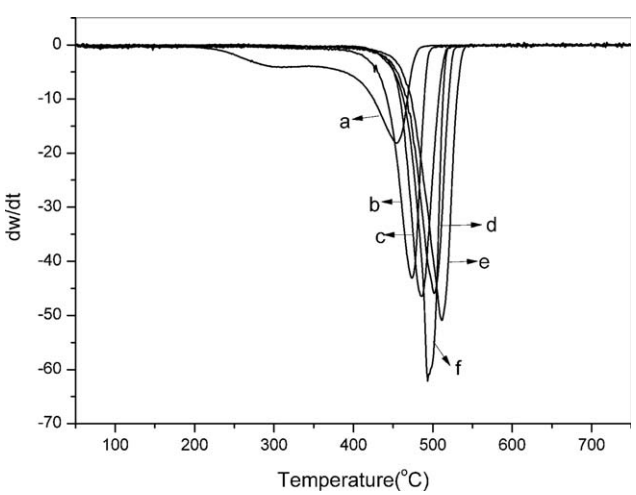

Figure 6 DTG curves under nitrogen flow of (a) sample HE8 (22.1 wt % MMT), (b) sample HE9 (17.9 wt % MMT), (c) sample HE10 (14.2 wt % MMT), (d) sample HE11 (10.8 wt % MMT), (e) sample HE13 (7.0 wt % MMT), and (f) sample neat PE.

TABLE IV
A Summary of Conditions and Results of Ethylene Polymerization with OMMT/Et[Ind]$_2$ZrCl$_2$ Under Different Reaction Conditions in Hexane and Toluene

Entry	Solvent	T (°C)	t (min)	Yield (g)	MMT (wt %)[a]	A ($\times 10^6$g/mol h)	T_m (°C)
HE1	Hexane	50	5	1.44	14.5	5.41	132.1
HE2			10	1.68	11.3	3.14	132.8
HE3			20	2.99	9.1	2.80	132.4
HE4			30	4.05	7.4	2.53	133.3
HE5			45	4.28	6.7	1.78	133.2
HE6			60	5.08	5.9	1.59	132.7
HE7			120	10.04	2.7	1.57	133.6
HE8	Hexane	30	15	0.60	22.1	0.72	132.3
HE9			30	1.21	17.9	0.72	132.9
HE10			45	1.60	14.2	0.64	132.5
HE11			60	2.07	10.8	0.62	132.4
HE12			90	2.37	9.2	0.47	132.4
HE13			120	3.10	7.0	0.47	131.7
TE1	Toluene	50	5	2.13	7.8	7.73	133.0
TE2			10	2.31	5.0	4.18	132.8
TE3			20	2.70	4.1	2.45	133.2
TE4			30	3.22	3.6	1.95	132.1
TE5			45	3.53	3.3	1.42	132.4
TE6			60	4.03	3.0	1.30	132.7
TE7			75	4.81	2.6	1.24	132.8
TE8			120	11.97	1.1	1.87	132.9

Polymerization conditions: ethylene pressure = 0.5 MPa, V = 100 mL solvent, [Al]/[Zr] = 1000.
[a] Calculated by TGA at 600°C.

(493°C). This is generally ascribed to the presence of large acidic sites on the layer silicate (formed after Hoffmann degradation) in the highly filled PE composites, which catalyzes the polymer degradation. However, sample HE11 (10.8 wt % MMT) and sample HE13 (7.0 wt % MMT) show higher thermally stability than that of neat PE, which can be due to a physical barrier effect of the nanodispersed silicate layers in PE matrix. As a result, the contents of MMT in PE matrix have an important effect on the thermal stability of PE/OMMT nanocomposites.

GPC analysis

To determine the molecular weight of the polyethylene matrix, solvent extraction was carried out using xylene at refluxing temperature on four nanocomposite samples (entry HE9, HE11, TE6, and TE8 in Table IV). The extracted polymer samples were subjected to GPC measurement. The results are summarized in Table V, showing that the polymer matrixes are of high molecular weight and broad molecular weight distribution.

WAXD and TEM analysis

The structures of all PE/OMMT nanocomposites were investigated using WAXD, as shown in Figure 7. A comparison for the intensities of the WAXD peaks of different samples implied that the extent of the OMMT exfoliation was higher in hexane than that in toluene, which was the reverse order of the clay content in the polymer [Fig. 7(A–C)]. When hexane was as polymerization solvent, both the OMMT/Et[Ind]$_2$ZrCl$_2$ catalyst and the MAO co-catalyst were suspended in it (Fig. 2), and the active specimens existed in between the silicate layers of OMMT. Therefore, the polymer chains propagated in the well-defined confinement environment at the beginning of polymerization, and the polymer obtained from hexane was so little that the polyethylene chains could not exfoliate the silicate layers of OMMT. Thus, a very distinct d_{001} peak was detected from the polymer after 15 min at 30°C (entry HE8 with 22.1 wt % in Table III), as seen in Figure 7(Ba). When the content of MMT in PE matrix is between 2.7 wt % and 14.0 wt %, the PE hybrids produced from hexane have no diffraction peak in the low angular region apart from the strong diffractions related to the crystalline PE. It is interesting to note that the PE/OMMT hybrid produced from hexane (entry HE10 in Table III) with 14.2 wt % OMMT

TABLE V
Matrix Molecular Weight and Molecular Weight Distribution of Nanocomposites

Entry in table IV	M_n($\times 10^4$)	M_w($\times 10^5$)	M_w/M_n
HE9	5.1	1.7	3.40
HE11	4.5	1.8	3.92
TE6	4.5	1.9	4.17
TE8	4.4	1.6	3.68

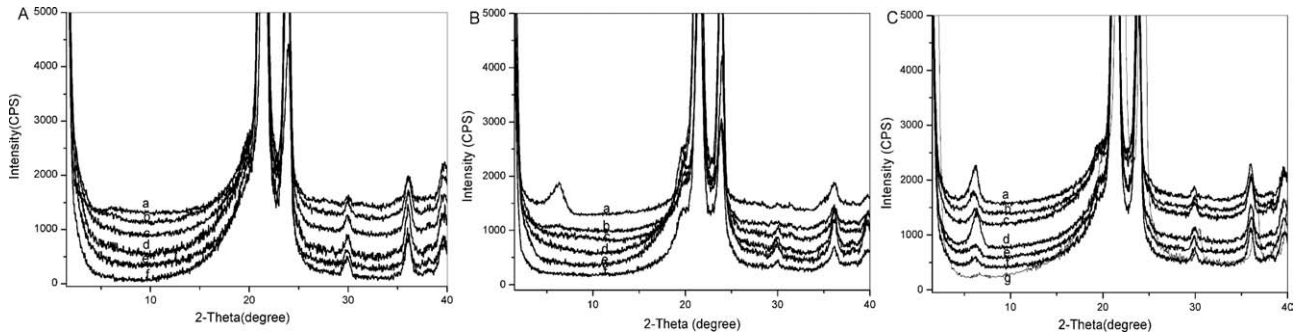

Figure 7 WAXD patterns of all PE-based hybrids (seen in Table III): (A) (a: sample HE1, b: sample HE3, c–g: sample HE4-HE7, respectively); (B) (a–f: sample HE8-HE13, respectively; (C) (a–e: sample TE1-TE5, f: sample TE7, g: sample TE8, respectively).

filling is completely diffraction signal-free (001) in the WAXD patterns. However, the polymers from toluene as solvent present a distinct diffraction peak at 2Θ angle from 5.4 to 6.0° [Fig. 7(C)], which is corresponding to a *d*-spacing of 1.47–1.64 nm for all the investigated composites, as listed in Table IV. This result is also in agreement with the reported literatures.[23] On the basis of above analysis, we can conclude that toluene as polymerization solvent has a better ability for dispersing OMMT/Et[Ind]$_2$ZrCl$_2$ in the presence of MAO than hexane does (seen in Fig. 3), inducing that active species of the catalyst were exposed in the gel formed by OMMT/Et[Ind]$_2$ZrCl$_2$ with MAO in toluene, which is supported by the numerical analysis of Zr contents in toluene as polymerization solvent in Table III (seen in dispersion and swelling of OMMT, MAO, Cat., Cat.+MAO in hexane or toluene section). That is to say, the growing polyethylene chains are mixed with the exfoliated silicate layers of OMMT in toluene, advocated by WAXD patterns of sample Cat.+MAO in toluene, as shown in Figure 3. Tritto and coworkers considered that the reaction of acid with the bound MAO present in the interlayer region of the clay caused the collapse of silicate layers in final polyethylene matrix.[23] But in our current research, all the quenching steps were in the same manner whether in hexane or in toluene. So we can consider that because the interaction force between the silicate layers of OMMT is larger than that between the polyethylene chains and the silicate layers, inherent immiscibility between the nonpolar polyethylene and the polar inorganic MMT in toluene results in collapse and low *d*-spacing parallel stacks of silicate layers in final PE matrix during the quenching step.

TEM images of sample HE3, HE10, and HE13 with different content of MMT prepared from hexane in Figure 8, show that a high degree of exfoliation of the clay is obtained, as testified in the presence of single layers and stacks containing few layers. Even though the amount of nanofiller is very high (>7 wt %), silicate layers of OMMT are well dispersed and disordered in the PE matrix. It can be concluded from both TEM and XRD measurements that exfoliated and highly filled PE/OMMT nanocomposites (>7 wt % MMT content) are obtained from hexane via *in situ* approach in slurry polymerization.

CONCLUSIONS

In summary, we demonstrate the *in situ* polymerization technique adopted through a slurry polymerization method and focus on understanding the interactions between OMMT and different polymerization solvents to obtain highly filled (>7.0 wt %) PE nanocomposites with a good dispersion of OMMT. Hexane and toluene are selected as solvents for comparative research of *in situ* polymerization. According to the Zr-content in the feed with different

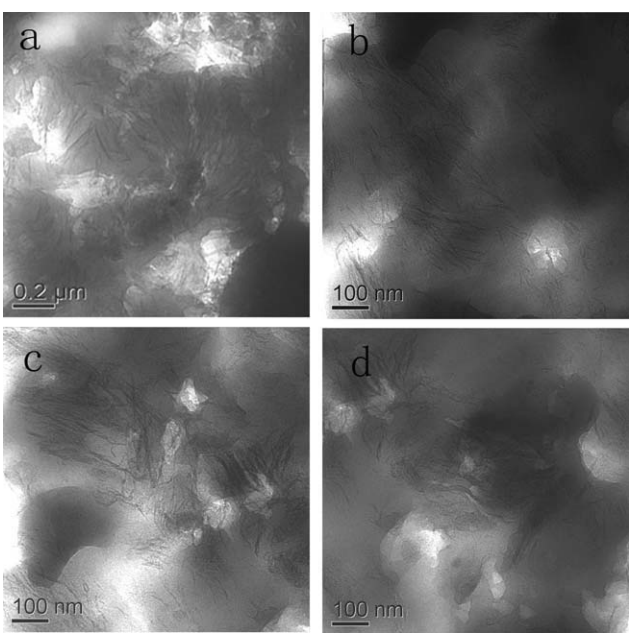

Figure 8 TEM images of (a) and (b) sample HE13, (c) sample HE10, and (d) sample HE3.

treatments, we can conclude that the OMMT/$Et[Ind]_2ZrCl_2$ catalyst in the presence of MAO are better dispersive and easier to expose in toluene than that in hexane, which affects ethylene polymerization kinetics. Under the similar reaction conditions, the maximum amount of absorbed C_2H_4 is larger in toluene than that in hexane. As the polymerization time increasing from 45 to 120 min, the amounts of absorbed C_2H_4 are hardly changed at all whether in toluene or in hexane. The WAXD pattern of OMMT/$Et[Ind]_2ZrCl_2$ in hexane with addition of MAO indicates most of the active sites exist in between the silicate layers of OMMT and polymer chains grow in the middle of them. However, when it occurs in toluene, most of them are exposed in the gel formed by the catalyst, facilitating the ethylene molecules freely approaching and resulting in the propagation of polymer chains in the gel. That is to say, PE chains are mixed with the silicate layers of OMMT in toluene. As a result, the catalytic activity of OMMT/$Et[Ind]_2ZrCl_2$ catalyst in toluene is higher than that in hexane at the early stage of polymerization. In addition, we observed that a longer polymerization time promoted a larger PE prepared in hexane, leading to an increased PE yield and the lower OMMT content in the nanocomposites. Thus, the larger PE chains separate the silicate layers of MMT. WAXD and TEM analysis imply that nanocomposites prepared from hexane solvent are with a good clay dispersion and a higher nanofiller content (above >7 wt %). In conclusion, only by selecting hexane as solvent in slurry polymerization, it is possible to obtain highly filled PE-based nanocomposites with a good exfoliation and dispersion of OMMT.

References

1. Kawasumi, M. J Polym Sci Part A: Polym Chem 2004, 42, 819.
2. Usuki, A.; Hasegawa, N.; Kato, M. Adv Polym Sci 2005, 179, 135.
3. Sinha Ray, S.; Okamoto, M. Prog Polym Sci 2003, 28, 1539.
4. Alexandre, M.; Dubois, P. Mater Sci Eng R 2000, 28, 1.
5. Ma, J. S.; Qi, Z. N.; Hu, Y. L. J Appl Polym Sci 2001, 82, 3611.
6. Pinnavaia, T. J.; Beall, G. W. Polymer-Clay Nanocomposites; Wiley: New York, 2001.
7. Manias, E.; Touny, A.; Wu, L.; Strawhecker, K.; Lu, B.; Chung, T. C. Chem Mater 2001, 13, 3516.
8. Bergman, J. S.; Chen, H.; Giannelis, E. P.; Thomas, M. G.; Coates, G. W. Chem Commun 1999, 21, 2179.
9. Heinemann, J.; Reichert, P.; Thomann, R.; Mülhaupt, R. Macromol Rapid Commun 1999, 20, 423.
10. Sun, T.; Garce's, J. M. Adv Mater 2002, 14, 128.
11. Alexandre, M.; Dubois, P.; Sun, T.; Garces, J. M.; Jérôme, R. Polymer 2002, 43, 2123.
12. Wang, Q.; Zhou, Z.; Song, L.; Xu, H.; Wang, L. J Polym Sci Part A: Polym Chem 2004, 42, 38.
13. Lee, D. H.; Kim, H. S.; Yoon, K. B.; Min, K. E.; Seo, K. H.; Noh, S. K. Sci Technol Adv Mater 2005, 6, 457.
14. Dubois, P.; Alexandre, M.; Jérôme, R. Macromol Symp 2003, 194, 13.
15. Ray, S.; Galgali, G.; Lele, A.; Sivaram, S. J Polym Sci Part A: Polym Chem 2005, 43, 304.
16. Liu, C. B.; Tang, T.; Wang, D.; Huang, B. T. J Polym Sci Part A: Polym Chem 2003, 41, 2187.
17. Liu, C.; Tang, T.; Huang, B. T. J Catal 2004, 221, 162.
18. Ho, D. L.; Briber, R. M.; Glinka, C. J. Chem Mater 2001, 13, 1923.
19. Barton, A. F. M. CRD Handbook of Solubility Parameters and Other Cohesion Parameters; CRC Press: FL, 1991.
20. Pinnavaia, T. J. Science 1983, 220, 365.
21. Ho, D. L.; Glinka, C. J. Chem Mater 2003, 15, 1309.
22. Choi, Y. S.; Ham, H. T.; Chung, I. J. Chem Mater 2004, 16, 2522.
23. Leone, G.; Bertini, F.; Canetti, M.; Boggioni, L.; Stagnaro, P.; Tritto, I. J Polym Sci Part A: Polym Chem 2008, 46, 5390.
24. Leone, G.; Bertini, F.; Canetti, M.; Boggioni, L.; Conzatti, L.; Tritto, I. J Polym Sci Part A: Polym Chem 2009, 47, 548.
25. Yang, K.; Huang, Y.; Dong, J. Y. Polymer 2007, 48, 6254.
26. Hauser, E. A. Colloid Chemistry, Alexander, J., Ed. 1953; Vol. 7, p 431950.
27. Slabaugh, W. H.; Hiltner, P. A. J Phys Chem 1968, 72, 4295.
28. Slabaugh, W. H.; Hanson, D. B. J Colloid Interface Sci 1969, 29, 460.
29. Slabaugh, W. H.; St Clair, A. D. J Colloid Interface Sci 1969, 29, 586.
30. Moraru, V. N. Appl Clay Sci 2001, 19, 11.
31. Brandruo, J.; Immergut, E. H. Polymer Handbook; 4th ed.; Wiley: New York, 1999.
32. Hanley, H. J. M.; Muzny, C. D.; Ho, D. L.; Glinka, C. J. Langmuir 2003, 19, 5575.